ACS OMEGA

Article

Cite This: ACS Omega 2019, 4, 11880−11887

http://pubs.acs.org/journal/acsodf

Recycling of Perovskite Films: Route toward Cost-Efficient and Environment-Friendly Perovskite Technology

Priyanka Chhillar, Bhanu Pratap Dhamaniya, Viresh Dutta, and Sandeep K. Pathak*

Centre for Energy Studies, Indian Institute of Technology Delhi, New Delhi 110016, India

ABSTRACT: Mixed organic−inorganic halide perovskite solar cells have reached unprecedentedly high efficiency in a short term. Two major challenges in its large-scale deployment is the material instability and hazardous lead waste. Several studies have identified that lead replacement with its other alternatives does not show the similar assurance. In this manuscript, we introduce the concept of recycling of the degraded perovskite film (PbI_2), gaining back the initial optoelectronic properties as the best possible solution to avoid lead waste. The simple recycling procedure allows the utilization of some of the most expensive (fluorine-doped tin oxide), primary energy-consuming (TiO_2), and toxic (Pb) parts of the solar cell, reducing the payback time even further. This addresses the major issues of instability and expensive toxic lead disposal, altogether. We have demonstrated the comparative study of feasibility of recycling in degraded perovskite films deposited by three different standard fabrication routes. Films fabricated via acetate route shows efficient recycling compared to the other routes, i.e., chloride and sequential deposition routes. Moreover, recycling in sequentially deposited films needs further optimization.

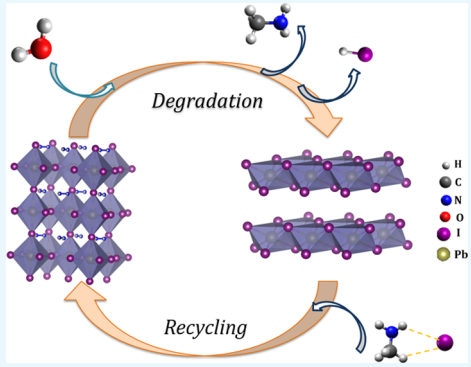

INTRODUCTION

In the last 5−6 years, mixed organic−inorganic halide perovskite materials such as methylammonium lead triiodide ($CH_3NH_3PbI_3$ or $MAPbI_3$) has been proved to be highly efficient light harvesters with photoconversion efficiency (PCE) exceeding 23%, comparable to other commercial technologies such as CIGS, CdTe, and Si.[1,2] This remarkable increase in PCE of metal halide perovskite has its root in the exceptional properties of high absorption coefficient ($\alpha = 5 \times 10^4$ cm^{-1} in red (1.7 eV)),[3] large charge diffusion length as long as 1 μm,[3,4] direct band gap of 1.55 eV at room temperature, and ambipolar charge transport due to small and balanced effective masses of charge carrier and high charge carrier mobilities.[3−5] Easy and cheap processability via spin coating, dip coating, and spray casting adds on to the merit.

The main hurdles to the commercialization of this technology despite all of the benefits mentioned above is the fact that $MAPbI_3$ is unstable when exposed to illumination, moisture, and high temperature.[3,6] Experimental evidences have proved that the presence of humidity is both beneficial and prejudicial depending on the circumstance. A restricted amount of humidity (∼30%) has an advantageous effect on the perovskite film properties during the crystallization phase,[7,6] improving the performance of the cell,[8,6] whereas exposure to ambient environment with humidity above 50% after crystallization has a detrimental effect on the perovskite solar cell.[9] Solving the issue of instability and degradation can conduce the technology to outcompete in photovoltaic marketplace.[10]

Another key challenge that needs to be addressed is the toxic Pb waste out of the damaged panels. Lead is cancerous and can disrupt the entire ecosystem if it enters the food chain.[2] The high cost of disposal of hazardous chemical waste (about $1.10/kg) adds on to the urge to uproot its usage.[2] According to Hailegnaw et al., about 30 t of Pb is required for 1 GW solar plant.[11] To resolve this issue, researchers worldwide have been trying hard to fabricate some efficient perovskite materials based on lead alternatives, but the idea has not seen the light of the day. Although there are various papers discussing about lead-free perovskite films, they fail to achieve similar optoelectronic properties. The highest efficiency with lead alternative is achieved using tin halide-based perovskite, which is 7%, but with even higher moisture sensitivity than $MAPbI_3$.[1212] Research worldwide on alternatives of Pb, using Sn, and Pb−Sn alloys had proved that complete elimination of Pb deteriorates the device performance.[13]

Cost analysis of perovskite solar cell modules with similar architecture has shown that a major fraction (around 40−60%) of the material embedded cost is borne by fluorine-doped tin oxide (FTO) substrate.[2] Owing to the high cost of FTO, researchers have tried to derive its alternatives and found that indium tin oxide/glass, poly(3,4-ethylenedioxythiophene):polystyrene sulfonate can be used but compromising the photoconversion efficiency.[14] Other significant contributors to material cost are the hole transporting material 2,2′,7,7′-tetrakis-(*N*,*N*-di-4-methoxyphenylamino)-9,9′-spirobifluorene (Spiro-OMeTAD) and gold top electrodes. According to Binek et al., the estimated costs of Spiro-OMeTAD and gold required are $40/$m^2$ and $25/$m^2$, respectively.[2] Some alternatives of Spiro-OMeTAD have proven to be quite

Received: April 13, 2019
Accepted: June 21, 2019
Published: July 9, 2019

DOI: 10.1021/acsomega.9b01053
ACS Omega 2019, 4, 11880−11887

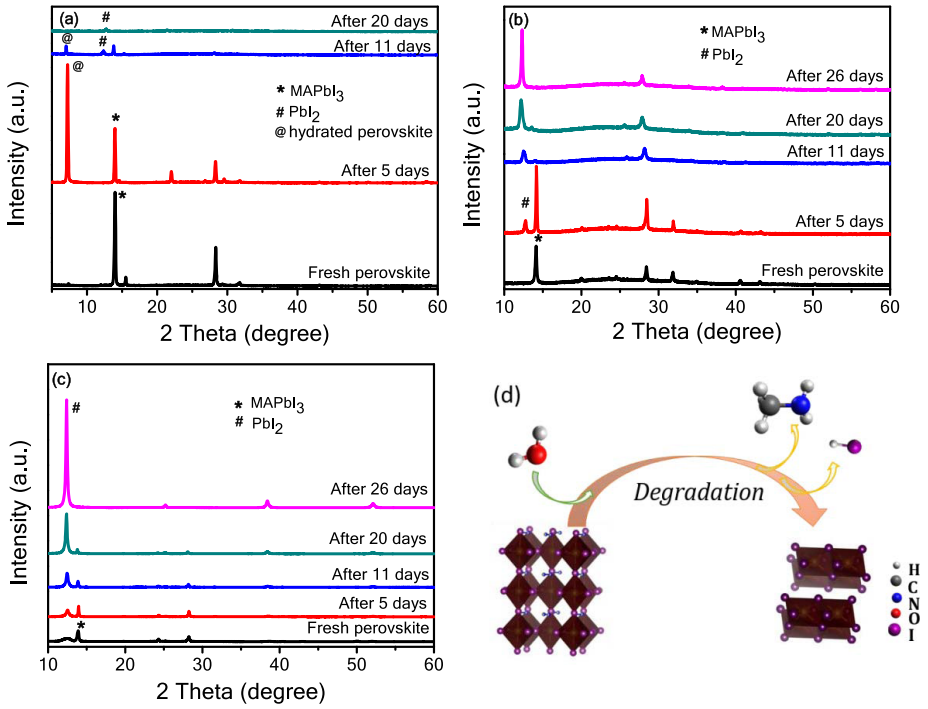

Figure 1. XRD patterns showing the degradation of (a) single-step chloride route, (b) single-step acetate route, and (c) sequential deposition route. (d) Crystal structure schematic showing the decomposition of $MAPbI_3$ into PbI_2 upon exposure to humidity.

promising, which can smoothly replace it on large-scale commercialization of the technology.[15,16] Expense of top electrodes can also be scaled down on large-scale production as it has been proved that there are competitive alternatives like silver that can replace them with not much compromise with efficiency.[17] Electron transport layer comprising compact titanium dioxide (TiO_2) although is not very cost-intensive, but its high-temperature sintering (~500 °C) consuming a large fraction of primary energy makes it a profound consideration. If this layer can be reused along with FTO, it serves the purpose of saving a lot of energy and time. Production of large-scale perovskite modules also involves essential cost of encapsulation, glass plates, interconnection busbars, sealant, laminating film, edge-sealing frame, a junction box, and wiring.[10] These, known as balance of module (BOM) components, constitute more than 70−80% of the total module cost.[10]

There have been some reports on the idea of reusing the FTO/TiO_2 layer for device fabrication dissolving the perovskite layer completely in dimethylformamide (DMF).[18,19] Xu et al. showed a recycling study, wherein they optimized thermal decomposition of $CH_3NH_3PbI_3$ film into PbI_2 on m-TiO_2-based architectures and then recycled the thermally decomposed PbI_2 film back to the perovskite.[20] In this manuscript, we discuss effectively the recycling of perovskite film in which we do not scratch out the perovskite film or dissolve anything but leave it as it is and recycle the existing degraded perovskite film.

In this manuscript, we have shown that by recycling the perovskite film, we not only cut down the cost by half reducing the payback time, but also reused lead devising it less problematic for the ecosystem. The same lead can then be reused a number of times without loss of its optoelectronic properties. Recycling of the same film numerous times also reduces the cost of technology further as the same FTO along with compact TiO_2 layer can be reused without impacting the device performance much. This will move the technology a step ahead in the path of commercialization. Here, we study the feasibility of recycling process in perovskite films fabricated via different methods. It has been detected that perovskite films fabricated via different routes have different morphologies and crystal properties and hence different optoelectronic properties. Therefore, in this study, to analyze the feasibility of the recovery mechanism, the perovskite films deposited by single-step chloride, single-step acetate, and sequential deposition routes were degraded in ambient environment for 26 days under humidity ranging from 25 to 35%. Various structural and optical characterizations were done to examine the nobility of the idea. Recycling of the perovskite solar cell can also bring about a path to reuse BOM, channelizing the technology ahead of the game.

RESULTS AND DISCUSSION

Degradation of $MAPbI_3$ Perovskite. This is a well-noted fact that sensitivity of $MAPbI_3$ perovskite to moisture is the biggest challenge, which needs to be urgently addressed. Exposure to moisture and sunlight leads to the complete corrosion of $MAPbI_3$ into PbI_2. $MAPbI_3$ in the presence of excess H_2O dissociates into methylammonium iodide (MAI) and PbI_2 (eq 1), and then after MAI decomposes into CH_3NH_2 and hydroiodic acid (HI) (eq 2).[21,22] On exposure to illumination and oxygen, HI breaks down further into its constituents generating I_2 (eqs 3 and 4)

$$CH_3NH_3PbI_3 \overset{H_2O}{\longleftrightarrow} CH_3NH_3I(aq)+PbI_2 \quad (1)$$

$$CH_3NH_3I(aq) \leftrightarrow CH_3NH_2(aq)+HI(aq) \quad (2)$$

$$2HI(aq) \overset{h\nu}{\leftrightarrow} H_2 \uparrow +I_2(s) \quad (3)$$

DOI: 10.1021/acsomega.9b01053
ACS Omega 2019, 4, 11880−11887

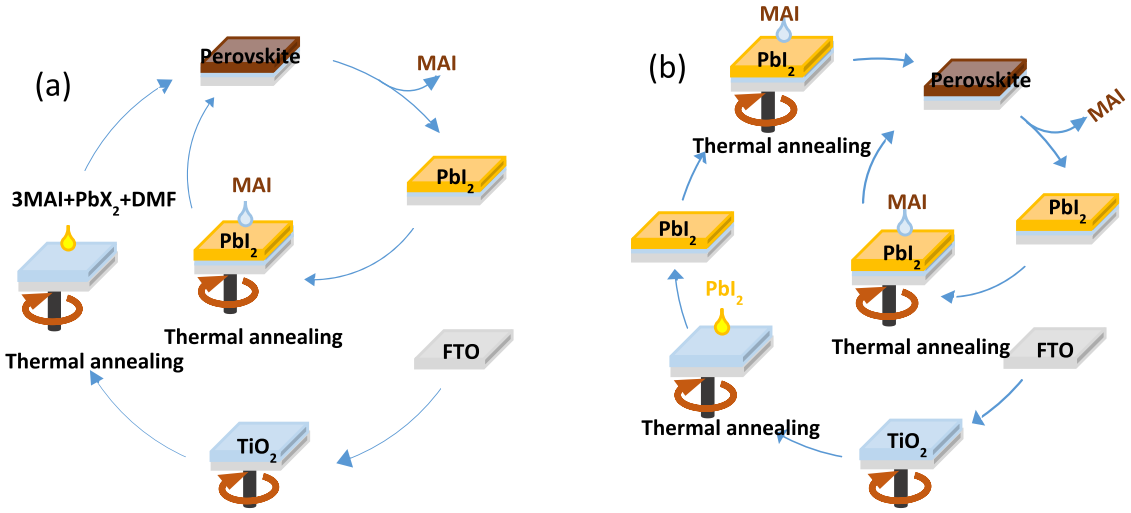

Figure 2. Schematic showing the recycling process for $MAPbI_3$ film deposited by (a) single-step chloride and single-step acetate route and (b) sequential deposition route.

$$4HI + O_2 \leftrightarrow 2I_2(s) + 2H_2O \quad (4)$$

It has been documented extensively as to how different fabrication routes lead to perovskite films with varying optoelectronic properties and hence different device efficiencies.[23] To prove the fact that the decomposition byproduct is PbI_2, degradation study of $MAPbI_3$ films fabricated via three different routes, i.e., single-step chloride, single-step acetate, and sequential deposition, was conducted. The X-ray diffraction (XRD) patterns in Figure 1a−c show the structural changes during degradation of the films fabricated by three different deposition routes.

The X-ray diffraction pattern indicates that the fresh perovskite films in all of the three routes show the characteristic peaks at 14.13°, 28.43°, and 31.84° corresponding to the (110), (220), and (114) lattice planes of $MAPbI_3$.[21,24,2521,24,25] The film fabricated via single-step chloride route shows an additional low-intensity peak at 15.6°, corresponding to the (100) plane of the $MAPbCl_3$ phase.[26−28] The formation of $MAPbCl_3$ intermediate phase in chloride-containing precursors has been reported in mixed-halide $MAPbI_{3-x}Cl_x$ perovskite.[27] It is detected in single-step chloride film that upon exposure to humidity, a hydrated phase is formed along with the perovskite phase, which is corresponded by the peak at around 7.2°.[29,30] On further exposure to humidity, the peak corresponding to PbI_2 starts to appear at around 12.6° along with the perovskite and hydrated perovskite peaks.[31] After prolonged exposure, perovskite and the hydrated peaks eventually disappear leaving behind only PbI_2 peak as can be ascertained from the XRD patterns shown in Figure 1a. Figure 1b,c shows the XRD patterns for single-step acetate and sequential deposition routes, respectively. Both of them show that on exposure to humidity, the PbI_2 peak starts to appear along with the characteristic perovskite peak. As the time of exposure increases, the intensity of the PbI_2 peak enhances and the perovskite peak is diminished, which ultimately disappears leaving behind just the PbI_2 peak. So, XRD analysis testifies the fact that in around 20 days of exposure to 25−35% humidity, $MAPbI_3$ is converted completely into PbI_2.

Thought behind recycling is that the remnant of degraded perovskite is PbI_2, which can easily be converted back into $MAPbI_3$ on reacting it with MAI. In this study, we have established a greater understanding on the feasibility of reverting PbI_2 into $MAPbI_3$, in terms of the optoelectronic properties and overall morphology of the film.

Recycling of $MAPbI_3$ Perovskite. In Figure 2, we show the schematic representation of the entire process steps involved in the degradation and recovery of $MAPbI_3$ films deposited via single-step chloride, single-step acetate, and sequential deposition routes.

To study the structural changes during degradation and to assess the degree of recovery by recycling process, we performed various structural and optoelectronic characterizations at different stages of degradation and after the recycling. In Figure 3, we show the X-ray diffraction pattern comparison of the fresh, degraded, and recycled perovskite films deposited via single-step chloride, single-step acetate, and sequential deposition routes.

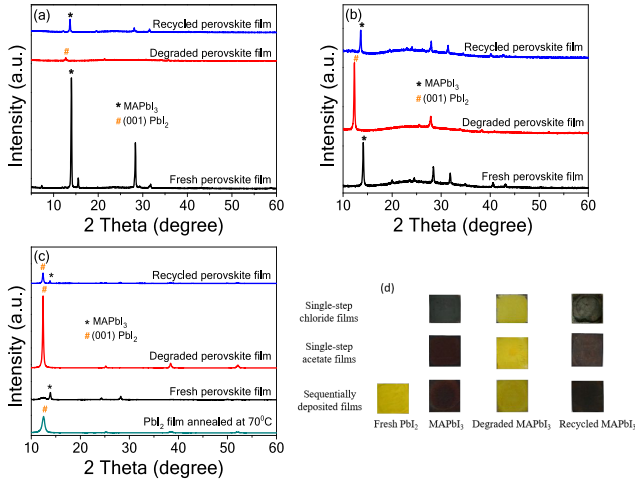

Figure 3. XRD patterns showing the fresh deposited perovskite film, degraded perovskite film left with PbI_2, and the recycled perovskite film for (a) single-step chloride, (b) single-step acetate, (c) sequential deposition route, and (d) the corresponding pictures of the films deposited by the three different routes at various stages of deposition, degradation, and recycling.

DOI: 10.1021/acsomega.9b01053
ACS Omega 2019, 4, 11880−11887

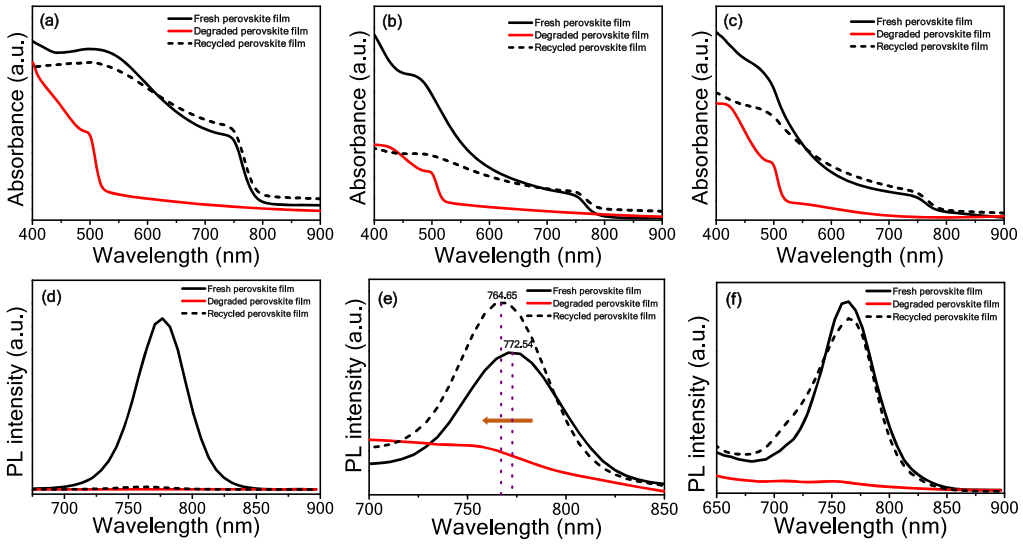

Figure 4. UV−vis spectra of $MAPbI_3$ perovskite film showing the absorption spectra of fresh deposited perovskite film, degraded perovskite film, and the recycled perovskite film: (a) single-step chloride, (b) single-step acetate, and (c) sequential deposition route. Photoluminescence (PL) spectra of $MAPbI_3$ perovskite film deposited by (d) single-step chloride, (e) single-step acetate, and (f) sequential deposition routes showing the fresh deposited perovskite film, degraded perovskite film containing PbI_2, and the recycled perovskite film.

In all three fabrication routes (i.e., single-step chloride, single-step acetate, and sequential deposition), upon exposure to ambient environment and under humidity for 26 days, characteristic perovskite peaks have diminished, while peaks pertaining to PbI_2 have appeared at around 12.6°, as ascertained from Figure 1.[31] Over time, the conversion of deep brown $MAPbI_3$ film into a yellow film shows that the perovskite film is now completely degraded, leaving behind a yellow film of PbI_2, as shown in Figure 3d. Experimental evidences have already proved the degradation of $MAPbI_3$ into PbI_2 on exposure to humidity.[21,32]

It is evident from Figure 3a that the characteristic peak intensity of fresh $MAPbI_3$ film deposited via the single-step chloride route is quite high, which signifies that the perovskite film is highly crystalline and well oriented. Then, after degradation of this film into PbI_2 peaks become less intense. This clearly shows that crystallinity is ablated upon degradation in single-step chloride films. Contrary to this in single-step acetate, the situation is transposed as can be seen from Figure 3b that upon exposure to humidity, peak intensity in the degraded film is slightly increased, thereby showing enhancement in the crystallinity of the film. XRD pattern of film deposited via sequential deposition shown in Figure 3c elucidates that upon exposure to ambient environment, crystallinity of the PbI_2 formed upon degradation of $MAPbI_3$ is drastically enhanced compared to the bare PbI_2 film annealed at 70 °C. These degraded samples were then processed through a recycling process by reacting the perovskite remains (i.e., PbI_2) with MAI. Interestingly, on coating the solution of MAI (10 mg/mL), the characteristic perovskite peaks reappeared with the disappearance of PbI_2 peak. For films fabricated from single-step chloride and single-step acetate routes, the PbI_2 peaks completely disappeared, confirming a complete recovery of the respective degraded perovskite films. However, on the other hand, in sequentially deposited films, peaks corresponding to both $MAPbI_3$ and PbI_2 are present in recycled film XRD pattern, indicating that PbI_2 is not completely consumed upon recycling, as seen in Figure 3c. It can also be seen in Figure 3c that there is a large amount of unconverted PbI_2 in the recycled film. It has been reported that a small percentage of remnant PbI_2 is advantageous for solar cell as it acts like a blocking layer between TiO_2 and perovskite inhibiting backinjection and recombination of electrons.[33] However, a higher amount of unconverted PbI_2 is not preferable as it deteriorates the device performance.

The UV−vis absorption measurements were conducted to investigate the optical properties of the perovskite films shown in Figure 4a−c. Optical absorption spectra of perovskite film fabricated via all of the three routes range from 400 to 800 nm, which is consistent with the typical absorbance spectra of $MAPbI_3$ reported previously.[21,24] After degradation, absorption intensity between 520 to 800 nm is observed to be decreased, whereas absorption in the range of 400 to 520 nm, which corresponds to the PbI_2 absorption range (band gap ≈ 2.4 eV) is retained.[33] Interestingly, degraded perovskite films regained their lost absorption onset to its entire range upon recycling. This is in good agreement with the results observed from the XRD measurements. In all of the films, the recycled film absorption baseline is slightly higher, suggesting that the films have become coarser over the time.

Steady state PL studies were carried out to assess the photoactivity of the perovskite films before and after recycling. Figure 4d−f shows the PL spectra corresponding to the fresh, degraded, and recycled perovskite films of single-step chloride, single-step acetate, and sequential deposition routes. The signature peak of $MAPbI_3$ perovskite is observed at around 776 nm for single-step chloride, 770 nm for single-step acetate, and 764 nm for sequential deposition.[21] It is observed that the PL intensity of the fresh perovskite film of single-step chloride is much higher than that of single-step acetate and sequentially deposited film. Note that the film thicknesses of all three films were maintained to a similar range. The observed higher photoactivity of the single-step chloride films can be attributed to large grain domains in the films in comparison to the other two routes (single-step acetate and sequential deposition).

In all three cases, once the perovskite films are degraded, their PL peak around 770 nm diminishes, corroborating the

DOI: 10.1021/acsomega.9b01053
ACS Omega 2019, 4, 11880−11887

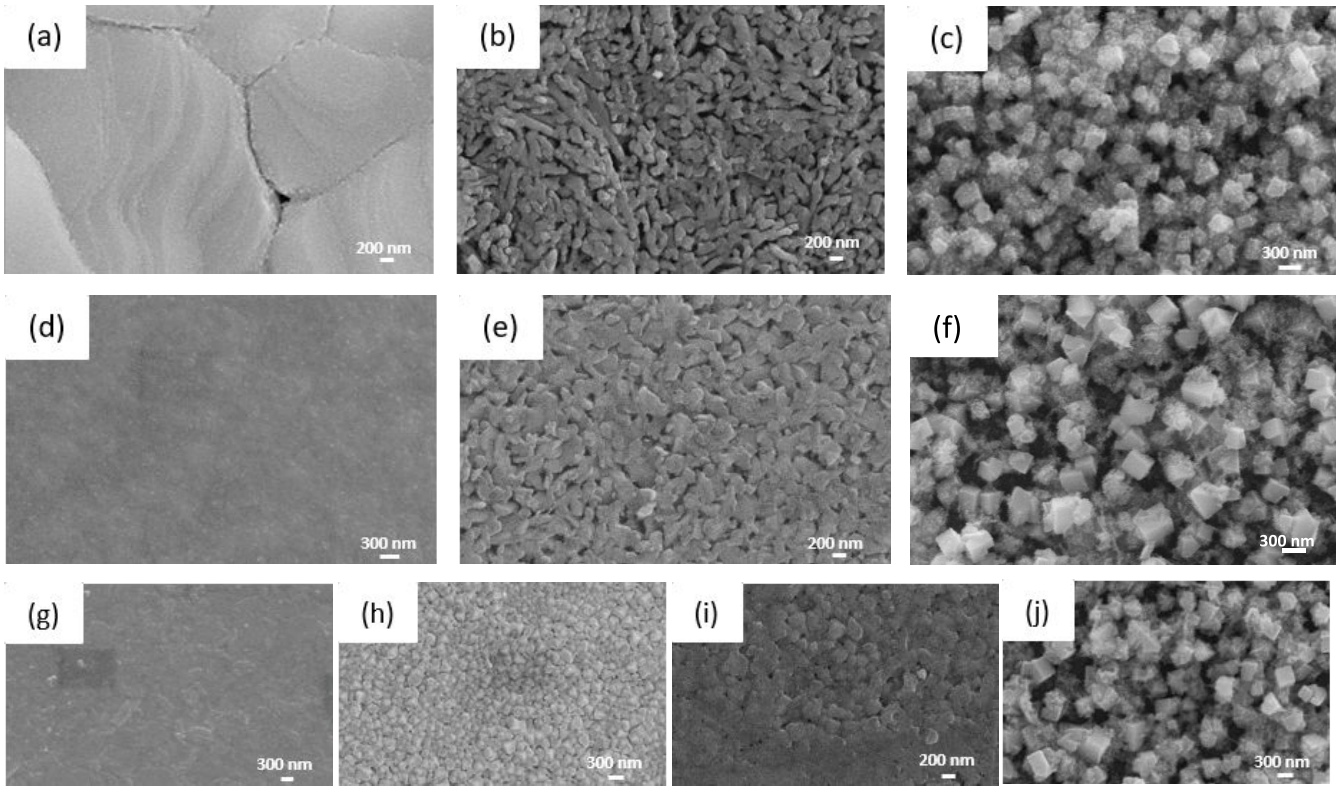

Figure 5. SEM images showing morphology of $MAPbI_3$ perovskite film deposited by single-step chloride route (a) fresh $MAPbI_3$, (b) degraded film, and (c) recycled film; $MAPbI_3$ perovskite film deposited by single-step acetate route (d) fresh $MAPbI_3$, (e) degraded film, (f) recycled film, (g) PbI_2 film annealed at 70 °C, (h) fresh perovskite film deposited by sequential deposition route, (i) degraded sequentially deposited film, and (j) recycled sequentially deposited film.

degradation of $MAPbI_3$ phase. The X-ray diffraction patterns of the respective degraded films have confirmed its composition as PbI_2 phase. By the recycling process, the same degraded perovskite film (i.e., PbI_2) is converted back to $MAPbI_3$ phase perovskite film. The yellowish degraded perovskite film (i.e., PbI_2) eventually becomes brown/black with reappearance of the signature PL peak at 770 nm of $MAPbI_3$ crystal.

However, PL peak intensity of recycled single-step chloride film is almost negligible compared to the fresh perovskite film from the same method. This confirms that the photoactivity of the original perovskite film fabricated via the single-step chloride route could not be recovered to a considerable degree after recycling. However, the XRD patterns confirmed the recovery of $MAPbI_3$ phase to a great degree. This is in concordance with the highly attenuated crystallinity of the film upon degradation, as observed from the XRD patterns, resulting in deterioration of photoactive properties upon recovery.

On the contrary, in the case of other two processing routes, i.e., single-step acetate and sequential deposition, as we show in Figure 4e,f, the photoactivities of the recycled films have fully recuperated to an extent of their respective original perovskite film. Interestingly, in the case of single-step acetate recycled film, PL emission intensity is slightly increased and a blue shift of about 6.04 nm is observed compared to the fresh single-step acetate film (Figure 4e). This could be due to passivation of electronic defect states, which is again beneficial accounting for superior optoelectronic properties.

Figure 4f shows that the characteristic perovskite PL peak is regained on recycling in sequential deposition case. However, the conversion of PbI_2 into perovskite is not complete in this particular case, as ascertained from XRD patterns. Despite that, the converted perovskite is showing photoactivity comparable to the fresh film. The increase in the crystallinity of the degraded film in sequential deposition explicates the fact behind regaining the photoactivity.

To explore the changes in the surface morphology of the films during the whole mechanism of degradation and recycling, scanning electron microscopy (SEM) was carried out (Figure 5a–j). The key behind getting a highly efficient solar cell lies in the fact that the film should be uniform pin hole-free and with good optoelectronic properties.[24,31,34]

Figure 5 shows the SEM images of films deposited via the three different routes at the various stages of deposition, degradation, and recycling. In Figure 5a, we show a perovskite film fabricated from single-step chloride method, which is pin hole-free and with larger grain domains of sizes in the order of micrometers. The intense PL emission that we observed in Figure 4d can be attributed to the large grain domains in the film, which might result in lower recombination rate.[7] Upon degradation of the single-step chloride film, the grain size in the leftover PbI_2 film is heavily reduced accompanied by pin holes. This explicates grounds for the observed decrease in crystallinity of the degraded film insured from the XRD pattern shown in Figure 3a. This decrease in the crystallinity also accounts for the aforementioned decrease in the PL intensity of the recycled perovskite compared to the fresh perovskite film in single-step chloride case. Release of H_2 and I_2 gases under illumination due to decomposition of HI is one of the chemical reactions that takes place while the degradation process in perovskite, could be the reason for the appearance of the voids in the degraded film of single-step chloride

DOI: 10.1021/acsomega.9b01053
ACS Omega 2019, 4, 11880−11887

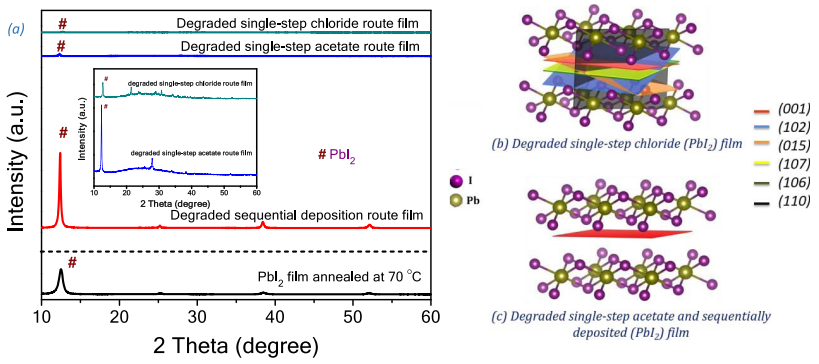

Figure 6. (a) Comparison of XRD patterns of the bare PbI_2 film annealed at 70 °C with those of the degraded films of single-step chloride, single-step acetate, and sequential deposition routes, i.e., PbI_2 (inset: single-step chloride, single-step acetate peaks on zoomed scale). Crystal structures of PbI_2 obtained from (b) degraded singe-step chloride film and (c) degraded single-step acetate and sequentially deposited film.

perovskite. Although introduction of MAI leads to transformation of PbI_2 into $MAPbI_3$ with increased domain size after recycling. In the case of single-step acetate, the domain size is increased after degradation compared to the fresh perovskite film. The aforementioned increase in the PL intensity of the recycled single-step acetate film is probably due to enhanced crystallinity of the degraded film (PbI_2). We have also shown a comparison of the morphology of the sequentially deposited film starting from the very first step of PbI_2 deposition to the recycled film (Figure 5g–j). SEM image of PbI_2 film annealed at 70 °C shown in Figure 5g shows large and diffused grains. Figure 5h depicts that upon conversion of this PbI_2 film into perovskite, the grain size is reduced, which is retained after degradation. During this whole process, the grains in the degraded film might have strongly oriented, which may account for the observed exceptional increase in the crystanillity of the degraded film witnessed from its XRD pattern (Figure 3c). It is already been constituted previously that degraded perovskite film morphology will govern the morphology and hence the optoelectronic properties of the recycled perovskite film. It is observed that upon degradation, the film morphology is deteriorating in single-step chloride and meliorating in the single-step acetate and sequentially deposited films. Recycling is thus more efficient in single-step acetate film without any loss in the optoelectronic property, while not much effective in single-step chloride as the film quality is worsened to an extent that cannot be retrieved. Similarly, sequential deposition route is also efficient in recycling; however, converting the entire degraded perovskite (i.e., PbI_2) film has proven difficult so far.

Importance of Decomposed PbI_2 Layer in Efficient Recycling. The process of recycling is analogous to the sequential deposition method, in which a predeposited PbI_2 is converted into perovskite films by introducing MAI.[35,24] The morphology and optoelectronic properties of the perovskite film grown by sequential deposition method are dependent on the morphology of PbI_2 film to a great extent, which was already established.[35] So, the feasibility of recycling will also depend upon the morphology and crystal properties of the degraded film, i.e., PbI_2. Therefore, it becomes critical to understand the crystal structure changes in the degraded PbI_2 films compared to fresh PbI_2.

Figure 6a shows the structural comparison of PbI_2 films collected after degradation of perovskites deposited via single-step chloride, single-step acetate, and sequential deposition routes. We also show X-ray spectra for a fresh PbI_2 film deposited from a freshly prepared PbI_2 solution in DMF deposited by spin coating on glass substrate, followed by annealing at 70 °C to draw a comparison with the various degraded PbI_2 films. XRD peaks at 2θ values 12.6°, 25.5°, 38.5°, and 52.2° corresponding to the (001), (002), (003), and (004) planes of hexagonal 2H polytype PbI_2 are recorded in the degraded films.[36] Degraded single-step chloride, single-step acetate, sequential deposition, and fresh film PbI_2 show preferred orientation along the (001) plane.[36] Degraded film of single-step acetate route shows similar crystal orientation to the fresh PbI_2film with much diminished peak intensity. In single-step acetate, there is one additional peak at 27.85° corresponding to the (109) plane of PbI_2 (JCPDS card 73-1287). The X-ray pattern of the degraded single-step chloride film shows peaks at 12.6°, 21.39°, 24.09°, 30.75°, 34.21°, 37.23°, 38.79°, 39.64°, and 52.47° corresponding to the (001), (005), (102), (015), (106), (107), (003), (110) and (004) planes (JCPDS card- 73-1752), as depicted in the crystal structure shown in Figure 6b. It can also be ascertained from Figure 6a that PbI_2 film obtained by degradation of sequentially deposited film is the best oriented film with enhanced crystallinity and retains an identical orientation to the fresh PbI_2 film.

The peak intensities in degraded single-step chloride film are the least among the other two, indicating a complete distortion of the crystal structure. Also, there are many very low-intensity peaks apparent in the XRD patterns indicating that the PbI_2 film produced upon degradation of films deposited via single-step chloride route are randomly oriented unlike single-step acetate and sequential deposition cases, as depicted in the crystal structures shown in Figure 6b,c.

Single-step chloride and single-step acetate routes show easy conversion to perovskite on introduction of MAI in the degraded films, as observed in Figure 3a,b. This is again in good agreement with the aforementioned observations. Since their crystallinity is greatly reduced compared to the fresh PbI_2 film, it is easy to convert these films back into perovskite. Contrary to this, crystallinity in sequentially deposited film is enhanced enormously upon degradation compared to the fresh PbI_2 film (Figure 6a). With the increased crystallinity, it becomes difficult for the MAI to penetrate deep inside the bulk of degraded PbI_2 film, resulting in incomplete conversion into perovskite (Figure 3c). However, if this highly crystalline film can be completely converted into perovskite, then it can lead to greatly augmented optoelectronic properties.

DOI: 10.1021/acsomega.9b01053
ACS Omega 2019, 4, 11880−11887

CONCLUSIONS

We have demonstrated that the recycling of degraded perovskite film is possible while retaining considerable order of PL efficiency and crystal structure. Our results show that the films deposited via single-step acetate route can be recycled more effectively than its single-step chloride and sequential deposition counterparts. Single-step chloride film is deteriorated to the extent that it cannot be recovered back to attain similar optoelectronic properties it exhibited initially. The PL intensity of the film from the single-step acetate route instead increased after recycling with a slight blue shift in its peak position compared to the fresh film, which shows rather advantageous effect on the film quality upon recycling for this particular case. Due to tremendous enhancement in the crystallinity of degraded PbI_2 film in sequential deposition with exposure to ambient environment, it cannot be completely transformed into $MAPbI_3$. Some method needs to be devised for the complete conversion of this highly crystalline PbI_2 film into perovskite, as that can lead to altogether superior grade of optoelectronic properties than its fresh counterpart. Fabrication of solar cells by reusing the degraded perovskite film itself will uproot the major environment lead contamination issue and will also reduce the fabrication cost and time, making the technology more agonistic.

EXPERIMENTS AND METHOD

Perovskite Solution Preparation. *Methylammonium Iodide (MAI) Preparation.* To prepare MAI, first, 24 mL of methyl ammine (MA 33 wt % in absolute ethanol, Sigma-Aldrich) was dissolved in 40 mL of ethanol (reagent grade). Then, 10 mL of hydroiodic acid (HI, Merck, 57% in water) was slowly added to this mixture while continuously stirring in an ice bath. After that, the solution was crystallized by keeping it undisturbed at 90 °C, followed by washing with diethyl ether three to four times. This solution was then redissolved in ethanol and kept in a refrigerator for recrystallization and subsequently dried.

Single-Step Acetate Route. To prepare the perovskite precursor solution, MAI and lead(II) acetate trihydrate ($Pb(Ac)_2{\cdot}3H_2O$, Merck) in 3:1 molar ratio were dissolved in anhydrous *N*,*N*-dimethylformamide (DMF, Sigma-Aldrich, 99.8%) at room temperature with a final mass concentration of 28 wt %.

Single-Step Chloride Route. To make the perovskite precursor solution, MAI and lead chloride ($PbCl_2$) were dissolved in DMF in 3:1 molar ratio at room temperature with a final mass concentration of 40 wt %.

Sequential Deposition Route. Lead iodide solution (PbI_2, 0.7 M) was prepared by dissolving in DMF adding 50 μL of HI per mL of solution under constant stirring. A solution of MAI in propan-2-ol (IPA) (10 mg/mL) was made at room temperature.

Perovskite Deposition. Glass slides were cleaned sequentially with labolene solution, followed by ultrasonication in deionized water, acetone, and IPA. This was done to remove all organic impurities on the glass slides. Single-step chloride perovskite films were deposited by spin-coating the precursor on the glass slides at 2000 rpm for 30 s in an air-filled dry box maintaining nearly 30% relative humidity. After spin coating, the films were annealed at 100 °C for 2.5 h.

Single-step acetate perovskite films were deposited by spin coating the precursor on the glass slides at 2000 rpm for 30 s in an air-filled dry box. After that, the films were left for drying for 10 min, followed by annealing at 100 °C for 5 min.

Sequential deposition route perovskite films were deposited by first spin coating the precursor solution of PbI_2 in DMF at 3000 rpm for 30 s. These films were then annealed at 70 °C for 30 min. After that, in the second step, 800 μL of MAI in IPA (10 mg/mL) solution was spin-coated on the PbI_2 film at 2000 rpm for 60 s, followed by annealing at 100 °C for 40 min for the complete conversion of PbI_2 into perovskite.

These $MAPbI_3$ perovskite films fabricated via three different routes were then left in the ambient environment for degradation to study the feasibility of the recycling process.

Recycling. Degraded perovskite films left with PbI_2 were recycled by spin coating 800 μL of MAI in IPA solution (10 mg/mL) at 2000 rpm for 60 s, followed by annealing at 100 °C for 40 min.

Measurement and Characterization. UV−vis absorption measurements were conducted using a PerkinElmer Lambda 1050 spectrophotometer. X-ray diffraction (XRD) measurements were carried out using a Rigaku Ultima IV diffractometer for structural analysis at a scan speed of 8°/min and step size of 0.02° using Cu Kα target. Photoluminescence was measured using an Agilent Cary Eclipse fluorescence spectrophotometer to examine the photoactivity of the samples. Surface morphology was observed using a scanning electron microscope (Zeiss EVO 50 & EVO 18 Special) operating at 20 kV.

AUTHOR INFORMATION

Corresponding Author

*E-mail: spathak@iitd.ac.in.

ORCID

Priyanka Chhillar: 0000-0003-0334-5605

Bhanu Pratap Dhamaniya: 0000-0003-1935-3597

Author Contributions

P.C. conducted all of the experiments required for the study and wrote the first draft. B.P.D. and V.D. contributed to the analysis, discussed this study, and provided valuable inputs. S.K.P. guided the entire study, structuring and editing the paper, and providing the rest with resources when necessary.

Notes

The authors declare no competing financial interest.

ACKNOWLEDGMENTS

The authors acknowledge Department of Science and Technology, India, for providing funding under grant number RP03396G. P.C. acknowledges IIT Delhi for providing Junior Research Fellowship. The authors acknowledge the Central Research Facility (CRF) and Nanoscale Research Facility (NRF) at Indian Institute of Technology Delhi for the SEM, XRD, and UV−vis measurements. They thank Prof. Josemon Jacob, CES, IIT Delhi, for allowing them to use his lab to conduct various experiments for this work.

REFERENCES

(1) He, M.; Zheng, D.; Wang, M.; Lin, C.; Lin, Z. High Efficiency Perovskite Solar Cells: From Complex Nanostructure to Planar Heterojunction. *J. Mater. Chem. A* **2014**, *2*, 5994−6003.

(2) Binek, A.; Petrus, M. L.; Huber, N.; Bristow, H.; Hu, Y.; Bein, T.; Docampo, P. Recycling Perovskite Solar Cells to Avoid Lead Waste. *ACS Appl. Mater. Interfaces* **2016**, *8*, 12881−12886.

DOI: 10.1021/acsomega.9b01053
ACS Omega 2019, 4, 11880−11887

(3) Giustino, F.; Snaith, H. J. Toward Lead-Free Perovskite Solar Cells. *ACS Energy Lett.* **2016**, *1*, 1233−1240.
(4) Stranks, S. D.; Eperon, G. E.; Grancini, G.; Menelaou, C.; Alcocer, M. J. P.; Leijtens, T.; Herz, L. M.; Petrozza, A.; Snaith, H. J. Electron-hole diffusion lengths exceeding 1 micrometer in an organometal trihalide perovskite absorber. *Science* **2013**, *342*, 341−344.
(5) Shi, D.; Adinolfi, V.; Comin, R.; Yuan, M.; Alarousu, E.; Buin, A.; Chen, Y.; Hoogland, S.; Rothenberger, A.; Katsiev, K.; et al. Low Trap-State Density and Long Carrier Diffusion in Organolead Trihalide Perovskite Single Crystals. *Science* **2015**, *347*, 519−522.
(6) Zhou, H.; Chen, Q.; Li, G.; Luo, S.; Song, T.-b.; Duan, H.-S.; Hong, Z.; You, J.; Liu, Y.; Yang, Y. Interface Engineering of Highly Efficient Perovskite Solar Cells. *Science* **2014**, *345*, 542−546.
(7) Eperon, G. E.; Habisreutinger, S. N.; Leijtens, T.; Bruijnaers, B. J.; van Franeker, J. J.; Dane, W.; Pathak, S.; Sutton, R. J.; Grancini, G.; Ginger, D. S.; et al. The Importance of Moisture in Hybrid Lead Halide Perovskite Thin Film Fabrication. *ACS Nano* **2015**, *9*, 9380−9393.
(8) Bass, K. K.; McAnally, R. E.; Zhou, S.; Djurovich, P. I.; Thompson, M. E.; Melot, B. C. Influence of Moisture on the Preparation, Crystal Structure, and Photophysical Properties of Organohalide Perovskites. *Chem. Commun.* **2014**, *50*, 15819−15822.
(9) Noh, J. H.; Im, S. H.; Heo, J. H.; Mandal, T. N.; Seok, S. I. Chemical Management for Colorful, Efficient, and Stable Inorganic−Organic Hybrid Nanostructured Solar Cells. *Nano Lett.* **2013**, *13*, 1764−1769.
(10) Song, Z.; Mcelvany, C. L.; Phillips, A. B.; Celik, I.; Krantz, P. W.; Watthage, S. C.; Liyanage, G. K.; Apul, D.; Heben, M. J. A technoeconomic analysis of perovskite solar module manufacturing with low-cost materials and techniques. *Energy Environ. Sci.* **2017**, *10*, 1297−1305.
(11) Hailegnaw, B.; Kirmayer, S.; Edri, E.; Hodes, G.; Cahen, D. Rain on methylammonium lead iodide based perovskites: possible environmental effects of perovskite solar cells. *J. Phys. Chem. Lett.* **2015**, *6* (9), 1543−1547.
(12) Noel, N. K.; Stranks, S. D.; Abate, A.; Wehrenfennig, C.; Guarnera, S.; Haghighirad, A.; Sadhanala, A.; Eperon, G. E.; Pathak, S. K.; Johnston, M. B.; et al. Lead-free organic−inorganic tin halide perovskites for photovoltaic applications. *Energy Environ. Sci.* **2014**, *7*, 3061−3068.
(13) Hao, F.; Stoumpos, C. C.; Chang, R. P. H.; Kanatzidis, M. G. Anomalous Band Gap Behavior in Mixed Sn and Pb Perovskites Enables Broadening of Absorption Spectrum in Solar Cells. *J. Am. Chem. Soc.* **2014**, *136*, 8094−8099.
(14) Sun, K.; Li, P.; Xia, Y.; Chang, J.; Ouyang, J. Transparent Conductive Oxide-Free Perovskite Solar Cells with PEDOT:PSS as Transparent Electrode. *ACS Appl. Mater. Interfaces* **2015**, *7*, 15314−15320.
(15) Malinauskas, T.; Saliba, M.; Matsui, T.; Daskeviciene, M.; Urnikaite, S.; Gratia, P.; Send, R.; Wonneberger, H.; Bruder, I.; Graetzel, M.; et al. Branched Methoxydiphenylamine-Substituted Fluorene Derivatives as Hole Transporting Materials for High-Performance Perovskite Solar Cells. *Energy Environ. Sci.* **2016**, *9*, 1681−1686.
(16) Peng, S.-H.; Huang, T.-W.; Gollavelli, G.; Hsu, C.-S. Thiophene and Diketopyrrolopyrrole Based Conjugated Polymers as Efficient Alternatives to Spiro-OMeTAD in Perovskite Solar Cells as Hole Transporting Layers. *J. Mater. Chem. C* **2017**, *5*, 5193−5198.
(17) Lee, M.; Ko, Y.; Min, B. K.; Jun, Y. Silver Nanowire Top Electrodes in Flexible Perovskite Solar Cells Using Titanium Metal as Substrate. *ChemSusChem* **2016**, *9*, 31−35.
(18) Huang, L.; Xu, J.; Sun, X.; Xu, R.; Du, Y.; Ni, J.; Cai, H.; Li, J.; Hu, Z.; Zhang, J. New Films on Old Substrates: Toward Green and Sustainable Energy Production via Recycling of Functional Components from Degraded Perovskite Solar Cells. *ACS Sustainable Chem. Eng.* **2017**, *5*, 3261−3269.
(19) Huang, L.; Hu, Z.; Xu, J.; Sun, X.; Du, Y.; Ni, J.; Cai, H.; et al. Efficient Electron-Transport Layer-Free Planar Perovskite Solar Cells via Recycling the FTO/Glass Substrates from Degraded Devices. *Sol. Energy Mater. Sol. Cells* **2016**, *152*, 118−124.
(20) Xu, J.; et al. In Situ Recycle of PbI_2 as a Step towards Sustainable Perovskite Solar Cells. *Prog. Photovoltaics* **2017**, *25*, 1022−1033.
(21) Dao, Q.; Tsuji, R.; Fujii, A.; Ozaki, M. Study on Degradation Mechanism of Perovskite Solar Cell and Their Recovering Effects by Introducing CH_3NH_3I Layers. *Org. Electron.* **2017**, *43*, 229−234.
(22) Li, D.; Liao, P.; Shai, X.; Huang, W.; Liu, S.; Li, H.; Shen, Y.; Wang, M. Recent Progress on Stability Issues of Organic−Inorganic Hybrid Lead Perovskite-Based Solar Cells. *RSC Adv.* **2016**, *6*, 89356−89366.
(23) Zhang, W.; Saliba, M.; Moore, D. T.; Pathak, S. K.; Hörantner, M. T.; Stergiopoulos, T.; Stranks, S. D.; Eperon, G. E.; Alexander-Webber, J. A.; Abate, A.; et al. Ultrasmooth Organic-Inorganic Perovskite Thin-Film Formation and Crystallization for Efficient Planar Heterojunction Solar Cells. *Nat. Commun.* **2015**, *6*, No. 6142.
(24) Li, H.; Li, S.; Wang, Y.; Sarvari, H.; Zhang, P.; et al. A Modified Sequential Deposition Method for Fabrication of Perovskite Solar Cells. *Sol. Energy* **2016**, *126*, 243−251.
(25) Oku, T. Crystal Structures and Related Perovskite Compounds Used for Solar Cells. *Solar Cells—New Approaches and Reviews*; IntechOpen, 2015.
(26) Sedighi, R.; Tajabadi, F.; Shahbazi, S.; Gholipour, S.; Taghavinia, N. Mixed-Halide $CH_3NH_3PbI_{3-X}X_X$ (X = Cl, Br, I) Perovskites: Vapor-Assisted Solution Deposition and Application as Solar Cell Absorbers. *ChemPhysChem* **2016**, *17*, 2382−2388.
(27) Tsai, H.; Nie, W.; Cheruku, P.; Mack, N. H.; Xu, P.; Gupta, G.; Mohite, A. D.; Wang, H. Optimizing Composition and Morphology for Large-Grain Perovskite Solar Cells via Chemical Control. *Chem. Mater.* **2015**, *27*, 5570−5576.
(28) Raga, S. R.; Jung, M.; Lee, M. V.; Leyden, M. R.; Kato, Y.; Qi, Y. Influence of Air Annealing on High Efficiency Planar Structure Perovskite Solar Cells. *Chem. Mater.* **2015**, *27*, 1597−1603.
(29) Christians, J. A.; Herrera, P. A. M.; Kamat, P. V. Transformation of the Excited State and Photovoltaic Efficiency of $CH_3NH_3PbI_3$ perovskite upon controlled exposure to humidified air. *J. Am. Chem. Soc.* **2015**, *137*, 1530−1538.
(30) Zhao, J.; Cai, B.; Luo, Z.; Dong, Y.; Zhang, Y.; Xu, H.; Hong, B.; et al. Investigation of the Hydrolysis of Perovskite Organometallic Halide $CH_3NH_3PbI_3$ in Humidity Environment. *Sci. Rep.* **2016**, *6*, No. 21976.
(31) Zhang, T.; Yang, M.; Zhao, Y.; Zhu, K. Controllable Sequential Deposition of Planar $CH_3NH_3PbI_3$ Perovskite Films via Adjustable Volume Expansion. *Nano Lett.* **2015**, *15*, 3959−3963.
(32) Leguy, M. A.; Hu, Y.; Campoy-quiles, M.; Alonso, M. I.; Weber, O. J.; Azarhoosh, P.; van Schilfgaarde, M.; Weller, M. T.; Bein, T.; Nelson, J.; et al. Reversible Hydration of $CH_3NH_3PbI_3$ in Films, Single Crystals, and Solar Cells. *Chem. Mater.* **2015**, *27*, 3397−3407.
(33) Cao, D. H.; Stoumpos, C. C.; Malliakas, C. D.; Katz, M. J.; Farha, O. K.; Joseph, T.; Kanatzidis, M. G. Remnant PbI_2, an Unforeseen Necessity in High-Efficiency Hybrid Perovskite-Based Solar Cells? *APL Mater.* **2014**, *2*, No. 091101.
(34) Zhao, Y.; Zhu, K. Solution Chemistry Engineering toward High-Efficiency Perovskite Solar Cells. *J. Phys. Chem. Lett.* **2014**, *5*, 4175−4186.
(35) Ko, H.; Lee, J.; Park, N. 15.76% efficiency perovskite solar cells prepared under high relative humidity: importance of PbI_2 morphology in two-step deposition of CH_3NH_3 PbI_3. *J. Mater. Chem. A* **2015**, *3*, 8808−8815.
(36) Burschka, J.; Pellet, N.; Moon, S. J.; Humphry-Baker, R.; Gao, P.; Nazeeruddin, M. K.; Grätzel, M. Sequential Deposition as a Route to High-Performance Perovskite-Sensitized Solar Cells. *Nature* **2013**, *499*, 316.

DOI: 10.1021/acsomega.9b01053
ACS Omega 2019, 4, 11880−11887